chemengineering

MDPI

Review

Review of the Application of Hydrotalcite as CO_2 Sinks for Climate Change Mitigation

David Suescum-Morales [1], José Ramón Jiménez [1,*] and José María Fernández-Rodríguez [2,*]

[1] Área de Ingeniería de la Construcción, Universidad de Córdoba, E.P.S. de Belmez. Avenida de la Universidad s/n, Belmez, E-14240 Córdoba, Spain; p02sumod@uco.es
[2] Área de Química Inorgánica, Universidad de Córdoba, E.P.S. de Belmez. Avenida de la Universidad s/n, Belmez, E-14240 Córdoba, Spain
* Correspondence: jrjimenez@uco.es (J.R.J.); um1feroj@uco.es (J.M.F.-R.)

Abstract: In recent decades, the environmental impact caused by greenhouse gases, especially CO_2, has driven many countries to reduce the concentration of these gases. The study and development of new designs that maximise the efficiency of CO_2 capture continue to be topical. This paper presents a review of the application of hydrotalcites as CO_2 sinks. There are several parameters that can make hydrotalcites suitable for use as CO_2 sinks. The first question is the use of calcined or uncalcined hydrotalcite as well as the temperature at which it is calcined, since the calcination conditions (temperature, rate and duration) are important parameters determining structure recovery. Other aspects were also analysed: (i) the influence of the pH of the synthesis; (ii) the molar ratio of its main elements; (iii) ways to increase the specific area of hydrotalcites; (iv) pressure, temperature, humidity and time in CO_2 absorption; and (v) combined use of hydrotalcites and cement-based materials. A summary of the results obtained so far in terms of CO_2 capture with the parameters described above is presented. This work can be used as a guide to address CO_2 capture with hydrotalcites by showing where the information gaps are and where researchers should apply their efforts.

Keywords: CO_2 sinks; calcined hydrotalcite; one-coat mortar; CO_2 curing

Citation: Suescum-Morales, D.; Jiménez, J.R.; Fernández-Rodríguez, J.M. Review of the Application of Hydrotalcite as CO_2 Sinks for Climate Change Mitigation. *ChemEngineering* **2022**, *6*, 50. https://doi.org/10.3390/chemengineering6040050

Academic Editors: Miguel A. Vicente, Raquel Trujillano and Francisco Martín Labajos

Received: 26 May 2022
Accepted: 28 June 2022
Published: 1 July 2022

1. Introduction

The incessant consumption of energy, which goes hand in hand with modern life in developed countries, has negative effects on the quality of the environment and ecosystems. These impacts, caused by greenhouse gases (GHGs), are leading many countries to adopt responsible environmental policies. Carbon dioxide (CO_2) is the dominant anthropogenic greenhouse gas (76%), responsible for global warming [1]. Before the industrial revolution (1760s), the CO_2 level was about 280 ppm [2], while today it could be considered at an average level of 400 ppm [3,4]. According to the International Energy Agency (IEA, 2017), the global mean temperature has increased by 1 °C above the preindustrial level due to anthropogenic greenhouse gas emissions [5]. The increase in global average temperature is expected to reach 1.5 °C by the end of 2040 [6,7], and it is therefore necessary to take measures to reduce these CO_2 levels.

To reduce these levels, two main carbon capture (CC) technologies are being presented [6,8]: (i) carbon capture, transport and storage technologies (CCS); and (ii) carbon capture and utilisation technologies (CCU). CCSs are primarily aimed at mitigating GHGs when fossil fuels are used for energy generation. CCS technologies are classified into three types: pre-combustion, post-combustion, and oxy-fuel combustion capture [6]. CCS technologies would remove around 20% of GHG emission by 2050 [9]. Captured CO_2 can be a source of recycled carbon, and CCU can provide more services and greater climate change savings than capturing and storing CO_2 underground [10]. The use of CO_2 gives an added value to these GHGs, which, together with the circular economy concept, can mitigate climate change [11,12]

Therefore, CO_2 capture is expected to play an important role in the commercialisation of future CCS technologies [13]. Many countries and research teams are considering various candidate processes and materials [14], such as absorption [15], adsorption [16,17]; membranes [18] and cryogenic distillation systems [19]. Solid sorbents (carbon, silica, calcium oxide, among others) are expanding as an emerging alternative for CO_2 capture, due to their great characteristics for such a task [20–22]. According to their temperature of use, solid sorbents can be classified as follows [23]: (a) low temperature (<200 °C) [24–27]; (b) intermediate temperature (between 200–400 °C) [28,29]; and (c) high-temperature (> 400 °C).

Hydrotalcites are brucite-like layered materials, that have been known for over 150 years with a general formula of $[M^{2+}_{1-x}M^{3+}_{x}(OH)_2]^{x+}(A^{n-})_{x/n}\cdot mH_2O$, where M^{2+} and M^{3+} represent divalent and trivalent cations, respectively, and A represents the interlayered anion [30–35]. Hydrotalcites are known in the bibliography as LDHs (Layered double hydroxides). The layer charge is determined by the molar ratio, that is $x = M^{3+}/(M^{3+} + M^{2+})$, and it varies between 0.2 and 0.4 [36–38]. The Mg_3AlCO_3 hydrotalcite is a type of LDH commonly found in nature. Reviewing the literature, a wide range of applications of these materials can be found [3]: catalytic applications [36,39–42], medical applications [43–46] as additives for polymers [47,48], for adsorption of pollutants [49–51], water decontamination [52,53], waste barriers [54–58], among various other applications. Several chemical companies (e.g., BASF, SASOL, Clariant, Kisuma Chemicals, Sakai Chemicals, etc.) produce several thousands of tonnes yearly, so it is an easily-available product [19]. Hydrotalcites, as such, are not good CO_2 absorbents due to poor basic properties and presence of entities that hinder CO_2 adsorption and are therefore subjected to thermal treatment (around 500 °C) to obtain nearly amorphous metastable mixed solid solutions known as calcined layered double hydroxides (CLDHs) [19]. In CLDHs, there is a loss of mass and a breakdown of its structure, forming an oxide, according to Equation (1) [59]:

$$Mg_6Al_2(OH)_{16}CO_3\cdot 4H_2O \rightarrow Mg_6Al_2O_9 + 12H_2O + CO_2 \quad (1)$$

The CO_2 emitted during calcination (Equation (1)) is identical to the CO_2 captured during the synthesis of hydrotalcite (Equation(2)):

$$Mg_6Al_2O_9 + 12H_2O + CO_2 \rightarrow Mg_6Al_2(OH)_{16}CO_3\cdot 4H_2O \quad (2)$$

Consequently, the CO_2 balance of the calcined hydrotalcite is 0 (Equations (1) and (2)). In this sense, all the CO_2 captured by the calcined hydrotalcite represents a negative CO_2 balance. This will reduce the carbon footprint of those materials to which calcined hydrotalcite is added.

Another characteristic of hydrotalcite is the memory effect, which allows the reconstruction of the original shape of hydrotalcite when it is in a humid environment and in the presence of CO_2. CLDHs in a CO_2 environment return to its initial state of LDHs [60–63]. The CO_2 capture balance by the hydrotalcite in its reconstruction is positive and hence the interest of using this material as a CO_2 capture material is very great (in the last decade) [64]. Nowadays, the challenge is to develop new types of hydrotalcites with higher CO_2 sorption capacities, higher sorption/desorption kinetics, and good stability throughout consecutive reutilisation cycles in similar operation conditions as those applied in a sorption-enhanced steam reforming process [65].

These hydrotalcites (in their LDH or CLDHs form) can also be found as additives to cement-based materials to improve resistance to chloride attack [66], durability [67–70] and even the use of LDH as additives to improve the thermal insulation of the intumescent fire retardant (IFR) coating [71]. Wu et al. [72] indicated that the structure regeneration of CLDHs in a cement paste environment had also been revealed [69]. After calcination, a large number of active sites produced what in favour of the improvement effect of CLDH on cement [72]. Since hydrotalcites may be incorporated into various building material mixtures, mortars, concretes and backfills, their application as accessible and affordable

materials is prospective [73–75]. However, research in the field of hydrotalcites and cement-based materials is still insufficient [72,76]. It is also difficult to find studies that add LDH or CLDH to alkaline-activated materials [77,78].

It is even more difficult to find studies in which CLDHs are used as additives in order to increase the CO_2 capture capacity of cement-based materials. Ma et al. [79] reported the adsorption of CO_3^{2-} by CLDH seven times faster than LDH due to the release of anions after calcination, which can be very beneficial for CO_2 capture. Suescum-Morales et al. [3,59] added different percentages of CLDH (calcined Mg_3AlCO_3) in a one-coat mortar in order to increase the CO_2 capture capacity. Adding 5% of calcined hydrotalcite increased the CO_2 capture capacity by 8.52% with respect to the reference mortar.

This paper presents a review of the application of hydrotalcites as CO_2 sinks. Different aspects were analysed: pH of the synthesis, the molar ratio (Mg/Al), the specific area, pressure, temperature and time in CO_2 absorption. A summary of the results obtained so far in terms of CO_2 capture with the parameters described above is presented. This work can be used as a guide to address CO_2 capture with hydrotalcites by showing where the information gaps are and where researchers should apply their efforts.

2. Calcined or Uncalcined Hydrotalcite to Capture CO_2?

The answer is immediate: calcined hydrotalcite or its use under high temperatures (around 400 °C so that the hydrotalcite becomes oxide and can be rebuilt in contact with CO_2). LDH are poor CO_2 adsorbents in their natural or unburned form, which is due to a poor basic property and the presence of entities that hinder CO_2 adsorption. Hence, they are subjected to thermal treatment to obtain nearly amorphous metastable mixed solid solutions (CLDHs) [19]. Figure 1 shows two diagrams representing what happens during the calcination of hydrotalcite of Mg_3AlCO_3 as shown (A) by W.J. Long et al. [77] and (B) by Lauermannová et al. [73]. Both schemes attempt to represent the collapse of the structure due to the loss of interlayer anions and moisture.

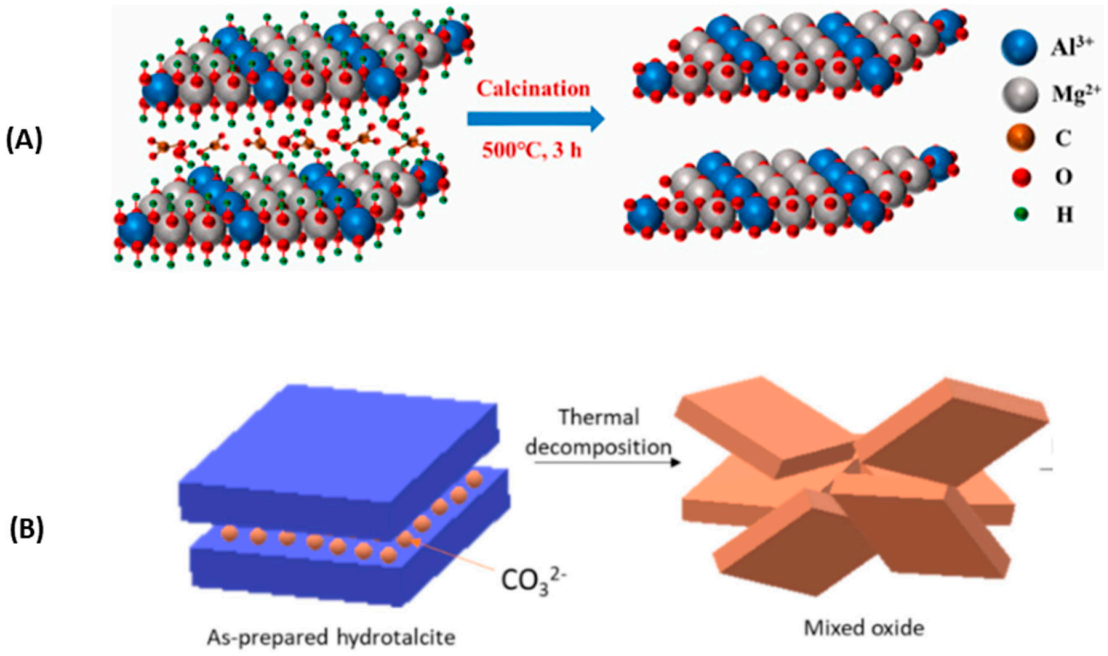

Figure 1. Structural changes of LDH after calcination according to adapted from W.J. Long et al. [77] (**A**) and Lauermannová et al. [73] (**B**) (open Access).

2.1. Thermal Behaviour of Hydrotalcite by TGA/DTA

LDH undergoes several stages until it reaches CLDHs. There is even research that attempts to explain this process in great detail and focuses on it alone [80,81]. It is very important to choose a suitable calcination temperature, avoiding it being too high (to avoid

higher energy consumption), or being too low (not producing the collapse of the structure and hindering a higher CO_2 capture). To distinguish the different stages, it is useful to rely on thermogravimetric analysis (TGA) and differential thermal analysis (DTA) carried out by Suescum-Morales et al. [33], shown in Figure 2. It should be noted that different variations in temperature ranges may be encountered, approximately as shown below.

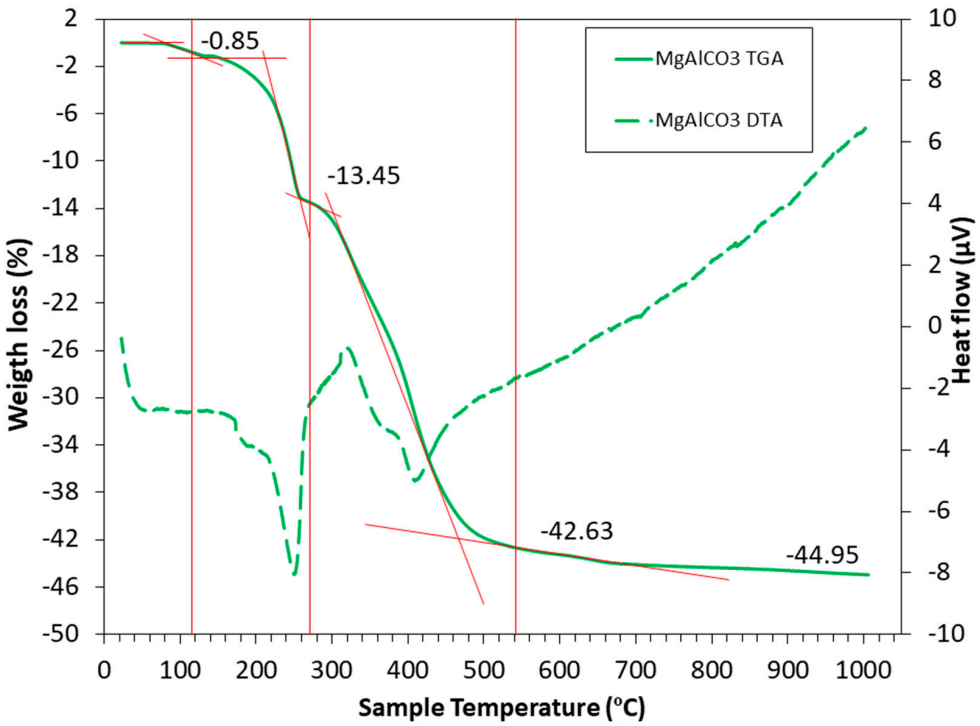

Figure 2. TGA (solid lines) and DTA (dotted lines) for commercial hydrotalcite of $MgAlCO_3$ [33].

First of all, a loss of humidity is observed, up to a temperature of about 105 °C. The second stage occurs from 105 to 270 °C, where the water hydration of the hydrotalcite structure is lost (leading to a decrease in basal spacing) [82–84]. There are authors who indicate that between 200 and 300 °C, the OH^- groups attached to Al^{3+} are lost [19]. The third stage, from 270 to 540 °C, is where the dehydroxilation of the hydrotalcite takes place and the loss of the carbonate anion of the interlayer in the form of CO_2 occurs. The layer structure collapses (Figure 1), and the LDH converts to a mixed-oxide MgO-like phase [85]. In the last stage, from 540 to 1000 °C, very small weight losses are observed, attributed to the loss of residual OH^- groups.

From the above, it can be seen that the calcination temperature affects the capacity to capture CO_2 in CLDHs. Different structural characteristics are presented in the different stages of thermal decomposition. From this analysis, the ideal calcination temperature of the hydrotalcite under study can be determined, which is characteristic and unique depending on the type of hydrotalcite. Most research indicates that the calcination temperature of a Mg-Al LDH is around 400 °C [86–88]. However, the performance of a TGA/DTA for each specific case would allow observing the exact calcination temperature. Therefore, specific experimental tests are necessary to further verify the influence of the calcination temperature on adsorption. This is discussed in the following sections of this review, using XRD, SEM/TEM, pH measurements in the synthesis, influence of molar ratio, and specific surface area measurements.

2.2. Thermal Behaviour of Hydrotalcite by XRD

The appropriate calcination temperature can also be determined by XRD temperature variation analysis. The thermal decomposition sequence of Mg-Al-CO_3 hydrotalcite is well documented. Miyata, 1980 and Hibino et al., 1995 [82,89] studied the XRD variation at

different temperatures, shown in Figure 4 (non-calcined, 150, 250, 350, 500, 850 and 1000 °C). The diffraction patterns of MgO can be identified between 400 °C and 850 °C, given the amorphous nature of Al_2O_3 at this temperature. For 900 °C the spinal phase ($MgAl_2O_3$) was formed. Given these experiences, the following chemical equations can be posed, with the different temperature ranges, to help us understand the process (Equations (3)–(5)):

$$Mg_6Al_2(OH)_{16}CO_3{\cdot}4H_2O \rightarrow Mg_6Al_2(OH)_{16}CO_3 + 4H_2O\ 100 < T < 250\ ^\circ C \quad (3)$$

$$Mg_6Al_2(OH)_{16}CO_3 \rightarrow 6Mg(Al)O + 8H_2O + CO_2 400 < T < 850\ ^\circ C \quad (4)$$

$$6MgO + Al_2O_3 \rightarrow MgAl_2O_4 + 5MgO\ 900 < T < 1000\ ^\circ C \quad (5)$$

Figure 3 shows the similar XRD obtained by several authors by calcination at 500 °C for different periods: firstly, the XRD obtained by W.J. Long et al. [77] (Figure 3a) shows how at a temperature of 500 °C for 3 h the layered structure collapses and also shows the production of mixed oxides. Figure 3b shows a similar result, but in this case using a calcination time of 2 h, and the same temperature (500 °C) [33]. This leads to a large saving of energy in the calcination of LDH, with a consequent lowering of the carbon footprint. Already, Z. Yang et al. [67] calcined at 500 °C for 3 h, obtaining a similar result. Even Q.Tao et al. [90] heated at 500 °C for 4 h, obtaining similar results (Figure 3c). Similar results in XRD were obtained by S.I. Garcés Polo et al. [91] for CLDH. None of the previous authors [33,67,77,91] indicated the amount of sample used in the calcination, which may have led to these observed differences. Although different calcination temperatures have been used with similar results, there are no economic studies of the cost of calcination; studies of this type, with times, temperatures and quantities of LDH to be calcined, would be very useful for these materials in industrial applications. It would also be very important to carry out a real carbon footprint calculation (UNE EN 15804:2012), which determines the real CO_2 sink capacity in each specific case (amount of hydrotalcite, type of furnace, etc.). Only two studies have been found that indicate the amount of hydrotalcite calcined (100 and 1 g respectively) [92,93]. Annotations of this type, i.e., what quantity is fed into the LDH kiln, are very important in order to maximise the efficiency of the calcination process.

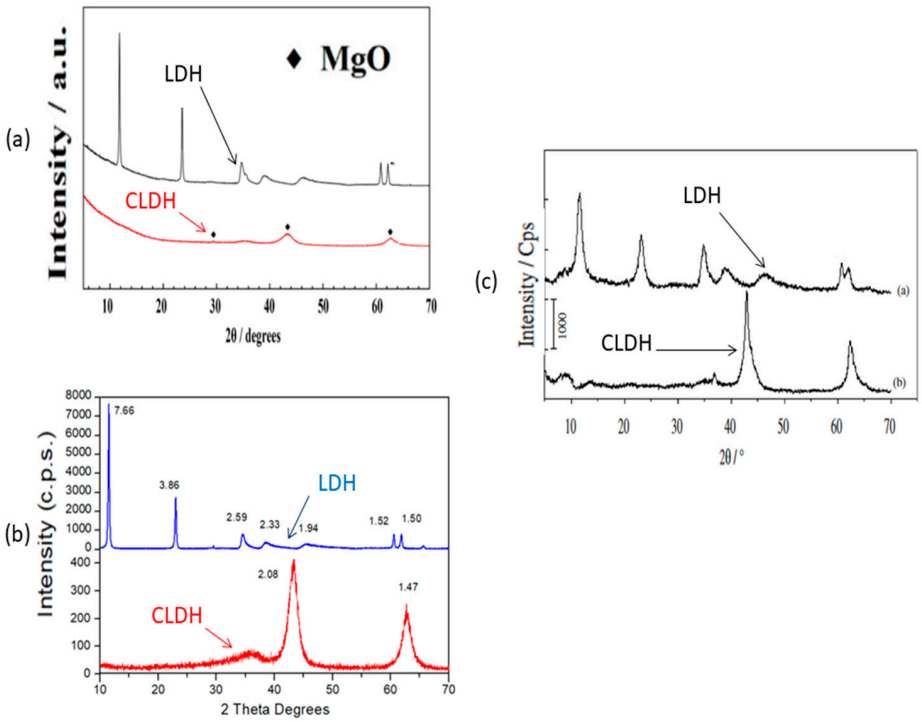

Figure 3. XRD patterns of (**a**) LDH and CLDH adapted from W.J. Long et al. [77]; (**b**) LDH and CLDH of Suescum-Morales et al. [33]; (**c**) LDH and CLDH adapted from Q.Tao et al. [90].

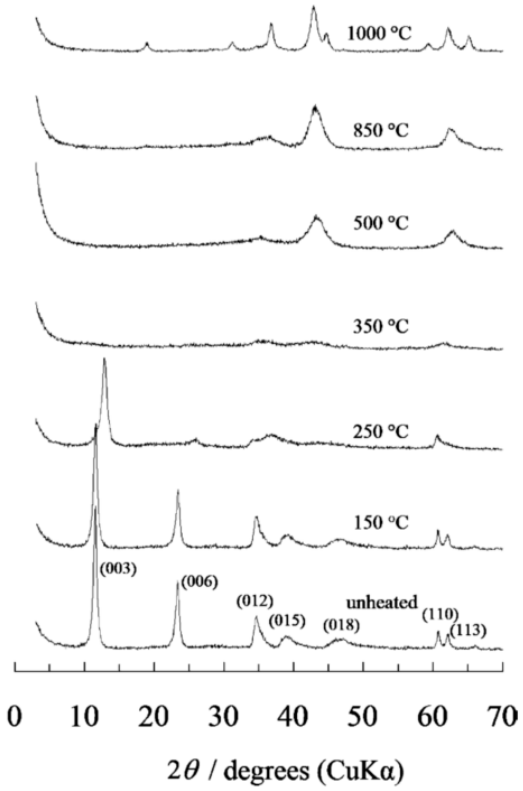

Figure 4. XRD of $MgAlCO_3$ formed between room temperature and 1000 °C [94].

2.3. Thermal Behaviour of Hydrotalcite by SEM/TEM

Figure 5a shows SEM images of commercial LDH and CLDH Mg-Al from W.J. Long et al. [77]. After 3 h at 500 °C, the structure collapses. A decrease in size was also observed. P. Cai et al. [95] obtained similar results (Figure 5b) with the same temperature and time of calcination. After 4 h at 450 °C on Mg-Al LDH, C. Geng et al. [96] observed a decrease in particle size, and the hexagonal shape was hardly noticeable (Figure 5c). No other studies using different temperatures (different at 500 °C) and calcination times have been found that show SEM images of LDH and CLDH. Studies along these lines could fill this information gap.

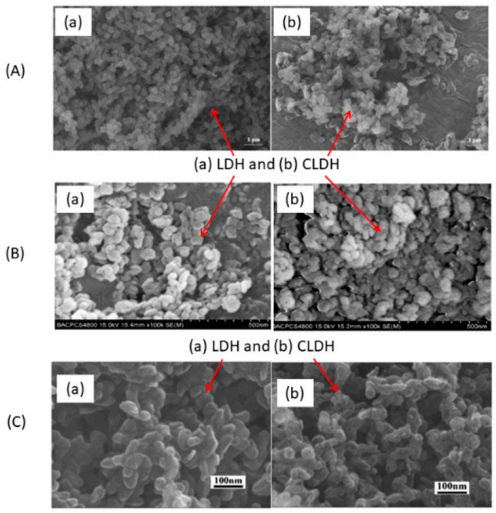

Figure 5. SEM images of LDH and CLDH Mg-Al of (**A**) adapted from W.J. Long et al. [77] and (**B**) adapted from P. Cai et al. [95] and (**C**) adapted from C. Geng et al. [96].

Figure 6A shows the TEM images of LDH and CLDH, after 2 h at 500 °C, obtained by Suescum-Morales et al. [33]. In CLDH, small pores were formed, attributable to the dehydration process, dehydroxilation of the OH^- groups, and to the decomposition of the interlayer carbonate. C Hobbs et al. [97] studied the evolution of a Mg-Al LDH under different temperatures using a rate of 10 °C/min (Figure 6B). At a temperature of 20 °C (LDH), they have a well-defined platelet shape; the porous structure is clearly visible at 850 °C. S Luo et al. [98] also obtained the same porous structure in CLDH, as shown in Figure 6C.

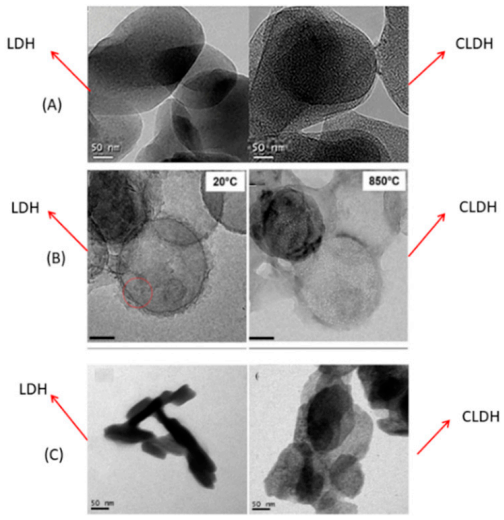

Figure 6. TEM images of LDH and CLDH Mg-Al of (**A**) Suescum-Morales et al. [33]; (**B**) adapted from C Hobbs et al. [97] (open access) and (**C**) adapted from S Luo et al. [98].

Different heating rates have been used in LDH calcination; a heating rate of 10 °C/min was used in Mg/Al LDH by several authors [99–102] and a heating rate of 5 °C /min was used by [103]. It is known that if the heating rate is slower, the thermal effects are better observed (better porous structure). However, if the ramp is slower, it takes more time and wastes more energy; if the heating is too fast, the porous structure will be worse. These differences should be extensively studied, both from an energy point of view (higher consumption and, therefore, higher carbon footprint produced by the kiln when the larger ramp is used), and from the point of view of the efficiency of the CLDH itself. Another very important aspect is the kinetics of LDH, which has been extensively discussed in other research [104,105].

3. Influence of the pH Used in the Synthesis in CO_2 Capture

Generally, LDH used for CO_2 capture has been synthesised by the coprecipitation method [33,34]. In this respect, Wang et al. [106] studied the effect of pH variation on the synthesis (coprecipitation method) in the range of 6.5–14. Subsequently, they studied the effect of the variation of this parameter on CO_2 capture. The pH that produced the best adsorption was 12 (23.76 mg/g). In other previous research, Wang et al. [88] indicated that the best pH value used for the synthesis of hydrotalcite oriented for CO_2 capture was between 10 and 12.

The crystallinity of the HT samples increases with the pH value of the synthesis, while the BET surface area decreases with increasing synthesis pH (in the range of 6.5–9 pH values). However, from a pH value of 10, the BET surface area increases suddenly, which can be seen in Figure 7, taken from Wang et al. [88].

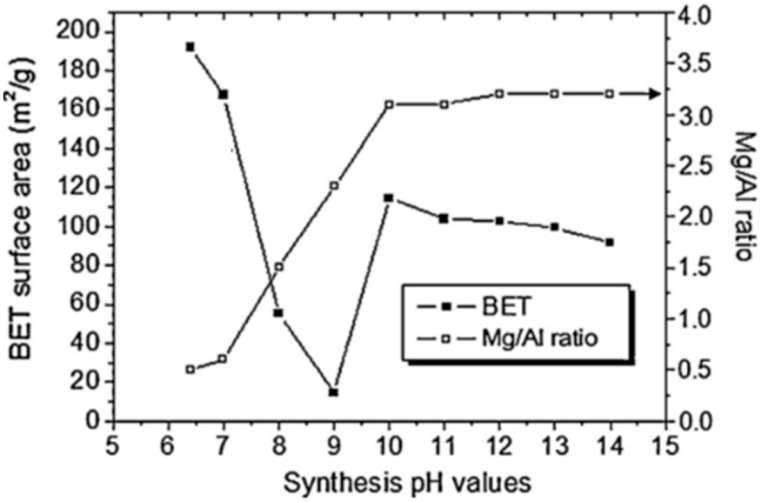

Figure 7. BET surface area and Mg/Al ratio as function of synthesis pH values adapted from Wang et al [88].

In other research studies, a pH of 7 was used by León et al. [25] and Rossi et al. [27], a pH of 9 was used by Torres-Rodriguez et al. [26], and a pH of 8 by Suescum-Morales et al. [33]. In summary, we must take into account that the pH value in the synthesis is fundamental in the development of the morphology, porous structure, as well as in the chemical composition (Mg/Al ratio).

4. Influence of the Molar Ratio (Mg/Al) of Its Main Elements in CO_2 Capture

The properties of LDH are also strongly influenced by the M^{2+}/M^{3+} ratio, cation type and anion type. For a higher capture capacity of CO_2, large interlayer spacing, high layer charge density and a greater number of basic sites are desirable. A high Al content increases the density, but decreases the layer spacing. A high Mg content increases the number of basic sites. In the consulted bibliography, optimal Mg/Al ratios are considered to vary from 1:1 to 3:1 [19,106–109].

Kim et al. [110] studied the effect of high Mg/Al ratios on the CO_2 sorption with hydrotalcites prepared with the coprecipitation method using ratios between 3 and 30. The highest CO_2 capture capacity was obtained (407.9 mg/g) for an Mg/Al ratio of 20, using temperatures of 240 °C.

M. Salomé Macedo et al. [111] studied the influence of different Mg/Al ratios (from 2 to 20) to be used as CO_2 sorbents at high temperature. The best results were obtained for an Mg/Al ratio of 7 at 1 bar of pressure and 300 °C (71.3 mg/g). These authors indicated that, in general, one observes a gradual increase in the sorption capacity for the same synthesis pH with the increase in the Mg/Al ratio.

The relationship between the pH of the synthesis, the molar ratio and the specific surface area obtained is very important. For example, Kim et al. [110] obtained the highest surface area with a molar ratio of 3 (256 m^2/g^-). M. Salomé Macedo et al. [111] showed that the BET specific surface area and total pore volume of samples clearly depend on the Mg/Al molar ratio. Suescum-Morales et al. [33] showed that the higher the specific surface area, the higher the CO_2 capture capacity. Therefore, the specific surface area seems to be a very important factor in determining the CO_2 capture.

As a summary, it can be said that although the molar ratio is very important in terms of CO_2 capture, there are also many other factors that affect this parameter: the pH of the synthesis, the nature of the anion, pressure used, and absorption temperature, among others, are the most important.

5. Ways to Increase the Specific Area of Hydrotalcites

The extensive literature presented in this paper highlights the significant interest of researchers in using LDH and CLDH as CO_2 adsorbents. Several strategies have been implemented in order to increase the CO_2 capture capacities: replacing cations or anions [88], different preparation methods [112], calcination, working temperatures and pressures [113] and alkali doping [29,114], among others.

A good strategy would be to increase the specific surface area, as a larger specific surface area would lead to a higher CO_2 capture capacity. Wang et al. [115] intercalated long carbon-chain organic anions, and it increased the CO_2 capture capacity. This was due to the increase in the interlayer distance from 0.78 to 3.54 nm (Figure 8). A similar strategy was followed by Li et al. [116], except that in this case they used K_2CO_3 in the LDH precursor of Mg_3Al-stearate, again increasing the interlayer distance, and achieving a higher CO_2 capture capacity. A similar strategy was also followed by A. Hanif et al. [117].

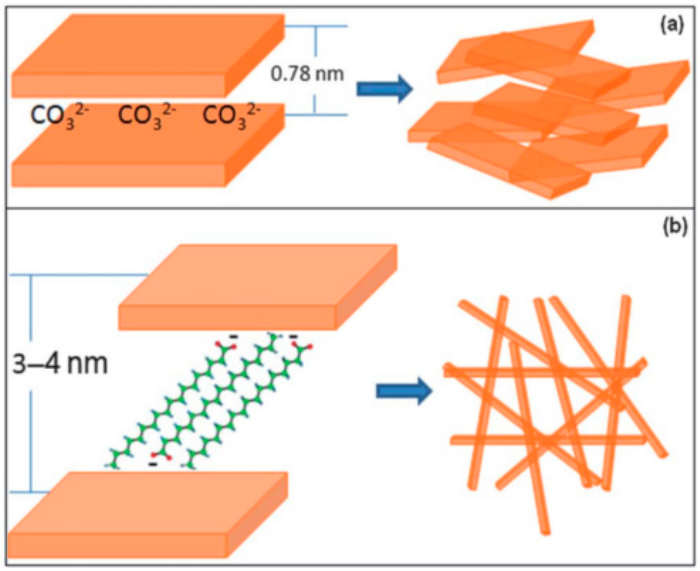

Figure 8. General schemes of the structural changes of (**a**) Mg_3Al-CO_3 and (**b**) with organic anions adopted from abstract of Wang et al [115].

Another way to increase the specific surface area would be to directly exfoliate the LDH in layers using bottom-up or top-down methods [118], although some authors indicate that the layers could be restacked after drying [119]. To avoid this, García-Gallastegui et al. [86] used graphene oxide as a support, where the negatively charged graphene oxide flakes were well dispersed in the positively charged LDH layers. Another strategy was followed by Othman et al. [120], who coated a $MgAlCO_3$ hydrotalcite with zeolites in order to increase the CO_2 capture capacity. K. Wu et al. [121] were the first to use mesoporous alumina to load LDH using the coprecipitation method, obtaining a large BET surface area (278–378 m^2/g).

A new method, called aqueous miscible organic solvent treatment (AMOST), uses solvents such as acetone and methanol to wash the LDH wet slurry and remove the intercalated water [119,122]. This method achieves larger surface areas and larger pore volumes [119]. Figure 9 shows the diagram of the synthetic process used for AMOST using acetone and K_2CO_3.

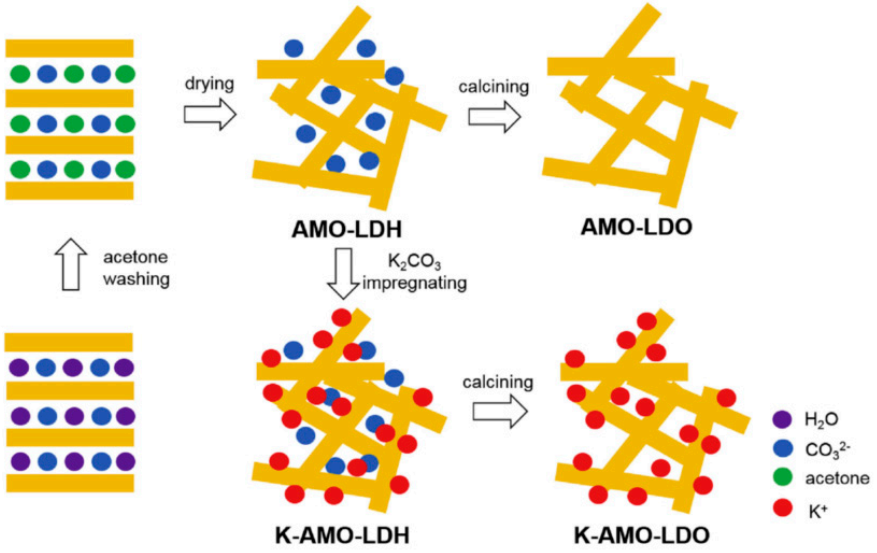

Figure 9. General scheme of synthetic process of AMOST method using by adopted from Zhu et al [122].

6. Pressure, Temperature, and Capacity in CO_2 Absorption and Use of CO_2 Captured

There are several parameters that can vary the CO_2 capture capacity of a hydrotalcite; among the most important are temperature and pressure [33]. Table 1 shows a comparison of the capture capacity of different types of hydrotalcite under different conditions.

Table 1. Maximum adsorption capacities of CO_2 for hydrotalcites reported in the literature.

Refs.	Type	LDH to CLDH?	Mg/Al Molar Ratio	Pressure (Atm.)	Temperature Isotherm (°C)	Capacity Adsorption (mg/g)
[29]	Alkali-modified (K and CS)	300 °C for 3 h	-	2	400	25.52
[38]	K promoted * Mg_3AlCO_3	LDH	-	16.50	400	28.60
[122]	* Mg_3AlCO_3 with treatment AMOST	450 °C for 3 h	3	1	400	30.58
[22]	K promoted * Mg_3AlCO_3	400 °C for 4 h	-	3.5	400	41.80
[64]	K promoted * Mg_3AlCO_3	400 °C for 3 h	-	10	400	25.68
[2]	K promoted commercial hydrotalcite	400 °C for 6 h	-	30	400	21.18
[117]	* Mg_3AlCO_3	450 °C for 10 h	2	13	350	44.95
[114]	K promoted * Mg_3AlCO_3	450 °C for 3 h	2.9	20	350	44.94
[28]	* Mg_3AlCO_3	400 °C for 4h	3	1	300	26.4
[7]	* Mg_3AlCO_3	400 °C for 2h	2	1	300	46.21
[91]	* Mg_3AlCO_3	500 °C for 4 h	3	43.42	300	144.32
[92]	Hydrotalcite of K-Na	650 °C for 6 h (100 g)	3 (K/Na ratio)	1.34	300	34.03
[112]	* Mg_3AlCO_3	400 °C for 2h	2	1	300	41.53
[116]	* K-Mg-Al	400 °C for 6 h	3	-	300	54.57
[86]	* Mg-Al with graphene oxide	400 °C for 4 h	-	-	300	12.84
[35]	Alkali metal (Na, Cs and K) with * Mg_3AlCO_3	300 °C for -h	2	0.15	300	21.12
[123]	K-loaded CNF supported hydrotalcite	500 °C for 4 h	-	1.1	250	62.27
[110]	* (Mg/Al = 20)	No information	20	1	240	407.97

Table 1. *Cont.*

Refs.	Type	LDH to CLDH?	Mg/Al Molar Ratio	Pressure (Atm.)	Temperature Isotherm (°C)	Capacity Adsorption (mg/g)
[88]	* Mg_3AlCO_3	-	3	1	200	23.32
[106]	* Mg_3AlCO_3	400 °C for 1 h	3.1	1	200	23.76
[23]	* Mg_3AlCO_3	400 °C for 4 h		1	200	39.60
[106]	* Mg_3AlCO_3	400 °C for 6 h	3	1	200	36.52
[124]	K promoted Gallium substituted hydrotalcite	400 °C	-	-	200	39.80
[121]	Mesoporous alumina with Mg-Al LDH	No	4	1	200	68.64
[26]	* Mg_3AlCO_3	550 °C for 1 h	3	1	80	93.72
[25]	* Mg_3AlCO_3	450 °C for 10 h	3	1	50	45.76
[27]	* Mg_3AlCO_3	400 °C for 1 h	3	1	50	40.04
[120]	* Mg-Al with coated zeolites	400 °C for 15 h	3	1	30	197.73
[93]	* Ni-Mg-Al	650 °C for 7 h (1 g)	-	1	20	70.62
[125]	* Cu-Al	600 °C for 75 min	3 (Cu/Al ratio)	1	20	20.54
[33]	* Mg_3AlCO_3	500 °C for 2 h	3	34.28	0	142.02
[34]	Organohydrotalcites TDD [1]	500 °C for 2 h	3	35	0	176.66

* Hidrotalcite of. [1] Tetradecanedioate anions.

As can be seen in Table 1, it is uncommon to use pressures higher than atmospheric pressure to measure CO_2 capture capacity, except in some research [2,22,29,38,64,91,92,114,117]. It is much more unusual to find research using high pressures and low temperatures (between 0 and 40 °C) [33,34]. At a pressure of 35 atm, an amount of 1.34 g of CLDH reduce CO_2 in 1 m^3 of air to preindustrial level [34]. Therefore, researchers have to pool their efforts to study CO_2 capture at high pressures and low application temperatures with calcined hydrotalcites.

Another very important factor to take into account will be the analysis of the reversibility conditions of CO_2 adsorption–desorption. For those materials in which it is reversible, these could be used to purify different gas streams in cyclic adsorption–desorption processes, as in the case of the use of CaO [21]. CaO could be used to capture CO_2 from thermal power plants or cement plants, to be stored and subsequently sold for use in different industrial processes. There is research in which CO_2 is used as a curing gas [11], capturing CO_2 (5.55 kg CO_2/t mix), improving mechanical properties and decreasing curing times (1 day in a CO_2 chamber is similar to 7 days in a conventional chamber), which can lead to an improvement in productivity. In addition, in order to avoid the inconvenience of using an accelerated carbonation chamber, an unprecedented strategy has been introduced, where an aqueous solution with injected CO_2 is used as kneading water, with very promising results [12]. In the case of irreversible processes, they could be used as CO_2 sinks, either alone or incorporated into other materials.

7. Combined Use of Hydrotalcites and Cement-Based Materials

The good and promising results obtained by the scientific community as adsorbents of hydrotalcites suggest the idea of incorporating them into construction materials, such as cement-based materials [66–70]. The ion exchange is the key feature that makes the use of LDH/CLDH in building materials attractive. These, together with the memory effect of CLDH, are the two suitable factors for the ion exchange and capture mechanism shown in Figure 10 [75].

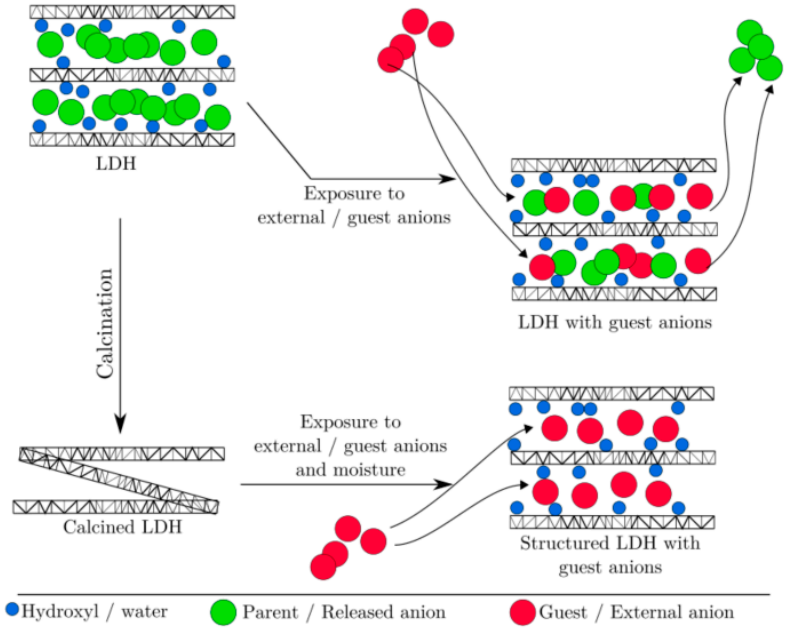

Figure 10. Schematic representation of the LDH/CLDH structure and ion exchange/captured mechanism represented by Zahid M. Mir [75] (open access).

In recent years, LDH/CLDH have emerged as a new class of engineering materials [75], which can aid in the corrosion control of concrete structures and potentially prolong their service life. Calcined hydrotalcite improves the durability of cement-base materials. One of the first findings mixing hydrotalcites with concrete dates back to 2004 [126]. In 2013, there were two very important contributions in this field [69,126].

This includes the use of LDH as an additive to improve the thermal insulation of the intumescent fire retardant (IFR) coating [71]. Wu et al. [72] indicated that the structure regeneration of CLDHs in a cement paste environment was also revealed [69]. After calcination, a large number of active sites produced were improving the effect of CLDH on cement [72]. Since hydrotalcites may be incorporated into various building materials mixtures, mortars, concretes and backfills, their applications as accessible and affordable materials is prospective [73–75]. However, research in the field of hydrotalcites and cement-based materials is still insufficient [72,76].

It is also difficult to find studies that add LDH or CLDH to alkaline activated materials [77,78]. Mixing LDH/CLDH in alkali-activated materials to improve the durability of these materials may be a very interesting field for the scientific community.

It is even more difficult to find studies in which CLDHs are used as additives in order to increase the CO_2 capture capacity of cement-based materials. Ma et al. [79] reported the adsorption of CO_3^{2-} by CLDH seven times faster than LDH due to the release of anions after calcination, which can be very beneficial for CO_2 capture. Suescum-Morales et al. [3,59] added different percentages of CLDH (Mg_3AlCO_3) in a one-coat mortar in order to increase the CO_2 capture capacity. Adding 5% of calcined hydrotalcite increased the CO_2 capture capacity by 8.52% with respect to the reference mortar. One m^2 of one-coat mortar with 5% of calcined hydrotalcites cleans 5540 m^3 of air [3]. The use of these one-coat mortars in building facades is a very promising strategy due to the large surface area exposed to the atmosphere. Studies along these lines should be reinforced to improve this information gap.

8. Conclusions

Application of hydrotalcites as CO_2 sinks and climate change mitigation is an emerging line of research. In this review, a guide on CO_2 capture by hydrotalcites is presented.

Firstly, the behaviour of hydrotalcites and the structural change from LDH to CLDH and their properties with the calcination of LDH are presented. After a review of the

literature, although the calcination temperatures are roughly similar, the times required to produce these changes, as well as the amount of hydrotalcite to be calcined, are somewhat diverse. Researchers must work together to clarify these factors so that they are not ambiguous data. These data would be very important since, for industrial use and a real application of these materials as CO_2 sinks, technical and economic calculations are necessary, which indicate the feasibility of using these products by companies. On the other hand, hydrotalcites can also be excessively calcined, with the consequent waste of energy (in time or temperature).

Secondly, the pH value in the synthesis is very important in the development of the morphology, porous structure, as well as in the chemical composition. The molar ratio (Mg/Al) is very important in terms of CO_2 capture, although there are also many other factors that affect this parameter: pH of the synthesis, nature of the anion, pressure used and absorption temperature.

It is also important to develop strategies that increase the specific surface area of hydrotalcites, as this is one of the most important factors in CO_2 absorption capacity. After a comparison of different studies (32 papers) on the capture capacity of LDH and CLDH, a gap in information on CO_2 capture capacities at high pressure and low temperature has been observed. Therefore, researchers have to pool their efforts to study CO_2 capture at high pressures and low application temperatures using calcined hydrotalcites.

It is very difficult to find studies in which CLDHs are used as additives in order to increase the CO_2 capture capacity of cement-based materials. The ion exchange and the memory effect of CLDH are key to the use of hydrotalcites as CO_2 capture additives in cement-based materials. Studies along these lines should be reinforced to improve this information gap and mitigate climate change.

Author Contributions: Conceptualization, D.S.-M. and J.M.F.-R.; Methodology, J.R.J.; writing—original draft preparation, D.S.-M.; writing—review and editing, J.M.F.-R. and J.R.J.; supervision, J.M.F.-R.; project administration, J.M.F.-R. and J.R.J. All authors have read and agreed to the published version of the manuscript.

Funding: This research has been supported from the Andalusian Regional Government, Spain (UCO-FEDER 20 REF. 1381172-R).

Data Availability Statement: Not applicable.

Acknowledgments: D. Suescum-Morales also acknowledges funding from MECD-Spain (http://www.mecd.gob.es/educacion-mecd/) FPU 17/04329 (accessed on 1 April 2022). The authors wish to thank the IE 57164 project for the implementation and improvement of scientific and technological infrastructures and equipment supported by the Andalusian Regional Government (FEDER 2011).

Conflicts of Interest: The authors declare no conflict of interest.

References

1. USEP Agency. Global Greenhouse Gas Emissions Data. 2022. Available online: https://www.epa.gov/ghgemissions/global-greenhouse-gas-emissions-data (accessed on 24 March 2022).
2. Van Selow, E.R.; Cobden, P.D.; Verbraeken, P.A.; Hufton, J.R.; Brink, R.W.V.D. Carbon Capture by Sorption-Enhanced Water−Gas Shift Reaction Process using Hydrotalcite-Based Material. *Ind. Eng. Chem. Res.* **2009**, *48*, 4184–4193. [CrossRef]
3. Suescum-Morales, D.; Cantador-Fernández, D.; Jiménez, J.R.; Fernández, J.M. Potential CO_2 capture in one-coat limestone mortar modified with Mg_3Al–CO_3 calcined hydrotalcites using ultrafast testing technique. *Chem. Eng. J.* **2021**, *415*, 129077. [CrossRef]
4. Martins, V.F.D.; Miguel, C.V.; Gonçalves, J.C.; Rodrigues, A.E.; Madeira, L.M. Modeling of a cyclic sorption–desorption unit for continuous high temperature CO_2 capture from flue gas. *Chem. Eng. J.* **2022**, *434*, 134704. [CrossRef]
5. IEA. Global Energy and CO_2 Status Report 2017. Glob. Energy CO_2 Status Rep. 2017. Available online: https://www.iea.org/publications/freepublications/publication/GECO2017.pdf (accessed on 1 April 2022).
6. Yadav, S.; Mondal, S. A review on the progress and prospects of oxy-fuel carbon capture and sequestration (CCS) technology. *Fuel* **2021**, *308*, 122057. [CrossRef]
7. Rocha, C.; Soria, M.; Madeira, L.M. Effect of interlayer anion on the CO_2 capture capacity of hydrotalcite-based sorbents. *Sep. Purif. Technol.* **2019**, *219*, 290–302. [CrossRef]
8. Bui, M.; Adjiman, C.S.; Bardow, A.; Anthony, E.J.; Boston, A.; Brown, S.; Fennell, P.S.; Fuss, S.; Galindo, A.; Hackett, L.A.; et al. Carbon capture and storage (CCS): The way forward. *Energy Environ. Sci.* **2018**, *11*, 1062–1176. [CrossRef]

9. Yadav, S.; Mondal, S.S. A complete review based on various aspects of pulverized coal combustion. *Int. J. Energy Res.* **2019**, *43*, 3134–3165. [CrossRef]
10. Christensen, T.H.; Bisinella, V. Climate change impacts of introducing carbon capture and utilisation (CCU) in waste incineration. *Waste Manag.* **2021**, *126*, 754–770. [CrossRef]
11. Suescum-Morales, D.; Kalinowska-Wichrowska, K.; Fernández, J.M.; Jiménez, J.R. Accelerated carbonation of fresh cement-based products containing recycled masonry aggregates for CO_2 sequestration. *J. CO2 Util.* **2021**, *46*, 101461. [CrossRef]
12. Suescum-Morales, D.; Fernández-Rodríguez, J.M.; Jiménez, J.R. Use of carbonated water to improve the mechanical properties and reduce the carbon footprint of cement-based materials with recycled aggregates. *J. CO2 Util.* **2022**, *57*, 101886. [CrossRef]
13. Boot-Handford, M.E.; Abanades, J.C.; Anthony, E.J.; Blunt, M.J.; Brandani, S.; Mac Dowell, N.; Fernández, J.R.; Ferrari, M.-C.; Gross, R.; Hallett, J.P.; et al. Carbon capture and storage update. *Energy Environ. Sci.* **2013**, *7*, 130–189. [CrossRef]
14. Jung, W.; Lee, J. Economic evaluation for four different solid sorbent processes with heat integration for energy-efficient CO_2 capture based on PEI-silica sorbent. *Energy* **2021**, *238*, 121864. [CrossRef]
15. Jung, W.; Lee, M.; Hwang, G.S.; Kim, E.; Lee, K.S. Thermodynamic modeling and energy analysis of a polyamine-based water-lean solvent for CO_2 capture. *Chem. Eng. J.* **2020**, *399*, 125714. [CrossRef]
16. Jung, W.; Park, J.; Won, W.; Lee, K.S. Simulated moving bed adsorption process based on a polyethylenimine-silica sorbent for CO_2 capture with sensible heat recovery. *Energy* **2018**, *150*, 950–964. [CrossRef]
17. Jung, W.; Park, S.; Lee, K.S.; Jeon, J.-D.; Lee, H.K.; Kim, J.-H.; Lee, J.S. Rapid thermal swing adsorption process in multi-beds scale with sensible heat recovery for continuous energy-efficient CO_2 capture. *Chem. Eng. J.* **2019**, *392*, 123656. [CrossRef]
18. Lee, S.; Kim, J.-K. Process-integrated design of a sub-ambient membrane process for CO_2 removal from natural gas power plants. *Appl. Energy* **2019**, *260*, 114255. [CrossRef]
19. Bhatta, L.K.G.; Subramanyam, S.; Chengala, M.D.; Olivera, S.; Venkatesh, K. Progress in hydrotalcite like compounds and metal-based oxides for CO_2 capture: A review. *J. Clean. Prod.* **2015**, *103*, 171–196. [CrossRef]
20. Wang, J.; Huang, L.; Yang, R.; Zhang, Z.; Wu, J.; Gao, Y.; Wang, Q.; O'Hare, D.; Zhong, Z. Recent advances in solid sorbents for CO_2 capture and new development trends. *Energy Environ. Sci.* **2014**, *7*, 3478–3518. [CrossRef]
21. Quesada Carballo, L.; Perez Perez, M.; Cantador Fernández, D.; Caballero Amores, A.; Fernández Rodríguez, J.M. Optimum Particle Size of Treated Calcites for CO_2 Capture in a Power Plant. *Materials* **2019**, *12*, 1284. [CrossRef]
22. Halabi, M.; de Croon, M.; van der Schaaf, J.; Cobden, P.; Schouten, J. High capacity potassium-promoted hydrotalcite for CO_2 capture in H_2 production. *Int. J. Hydrog. Energy* **2012**, *37*, 4516–4525. [CrossRef]
23. Kou, X.; Guo, H.; Ayele, E.G.; Li, S.; Zhao, Y.; Wang, S.; Ma, X. Adsorption of CO_2 on MgAl-CO_3 LDHs-Derived Sorbents with 3D Nanoflower-like Structure. *Energy Fuels* **2018**, *32*, 5313–5320. [CrossRef]
24. Williams, G.R.; O'Hare, D. Towards understanding, control and application of layered double hydroxide chemistry. *J. Mater. Chem.* **2006**, *16*, 3065–3074. [CrossRef]
25. León, M.; Díaz, E.; Bennici, S.; Vega, A.; Ordóñez, S.; Auroux, A. Adsorption of CO_2 on Hydrotalcite-Derived Mixed Oxides: Sorption Mechanisms and Consequences for Adsorption Irreversibility. *Ind. Eng. Chem. Res.* **2010**, *49*, 3663–3671. [CrossRef]
26. Torres-Rodríguez, D.A.; Lima, E.; Valente, J.S.; Pfeiffer, H. CO_2 Capture at Low Temperatures (30–80 °C) and in the Presence of Water Vapor over a Thermally Activated Mg–Al Layered Double Hydroxide. *J. Phys. Chem. A* **2011**, *115*, 12243–12250. [CrossRef] [PubMed]
27. Rossi, T.M.; Campos, J.; Souza, M.M.V.M. CO_2 capture by Mg–Al and Zn–Al hydrotalcite-like compounds. *Adsorption* **2015**, *22*, 151–158. [CrossRef]
28. Hutson, N.D.; Attwood, B.C. High temperature adsorption of CO_2 on various hydrotalcite-like compounds. *Adsorption* **2008**, *14*, 781–789. [CrossRef]
29. Oliveira, E.L.; Grande, C.A.; Rodrigues, A.E. CO_2 sorption on hydrotalcite and alkali-modified (K and Cs) hydrotalcites at high temperatures. *Sep. Purif. Technol.* **2008**, *62*, 137–147. [CrossRef]
30. Allmann, R. The crystal structure of pyroaurite. *Acta Crystallogr. Sect. B Struct. Crystallogr. Cryst. Chem.* **1968**, *24*, 972–977. [CrossRef]
31. Taylor, H.F.W. Crystal structures of some double hydroxide minerals. *Miner. Mag.* **1973**, *39*, 377–389. [CrossRef]
32. Miyata, S. The syntheses of hydrotalcite-like compounds and their structure and physico-chemical properties—I: The systems Mg^{2+}-Al^{3+}-NO^{3-}, Mg^{2+}-Al^{3+}-Cl^{-}, Mg^{2+}-Al^{3+}-ClO^{4-}, Ni^{2+}-Al^{3+}-Cl^{-} and Zn^{2+}-Al^{3+}-Cl^{-}. *Clays Clay Miner.* **1975**, *23*, 369–375. [CrossRef]
33. Suescum-Morales, D.; Cantador-Fernández, D.; Jiménez, J.; Fernández, J. Mitigation of CO_2 emissions by hydrotalcites of Mg_3Al-CO_3 at 0 °C and high pressure. *Appl. Clay Sci.* **2020**, *202*, 105950. [CrossRef]
34. Fernandez, D.C.; Morales, D.S.; Jiménez, J.R.; Fernández-Rodriguez, J.M. CO_2 adsorption by organohydrotalcites at low temperatures and high pressure. *Chem. Eng. J.* **2021**, *431*, 134324. [CrossRef]
35. Faria, A.C.; Trujillano, R.; Rives, V.; Miguel, C.; Rodrigues, A.; Madeira, L.M. Alkali metal (Na, Cs and K) promoted hydrotalcites for high temperature CO_2 capture from flue gas in cyclic adsorption processes. *Chem. Eng. J.* **2021**, *427*, 131502. [CrossRef]
36. Cavani, F.; Trifirò, F.; Vaccari, A. Hydrotalcite-type anionic clays: Preparation, properties and applications. *Catal. Today* **1991**, *11*, 173–301. [CrossRef]
37. Costantino, U.; Nocchetti, M.; Sisani, M.; Vivani, R. Recent progress in the synthesis and application of organically modified hydrotalcites. *Zeitschrift für Kristallographie* **2009**, *224*, 273–281. [CrossRef]

38. Ding, Y.; Alpay, E. Equilibria and kinetics of CO_2 adsorption on hydrotalcite adsorbent. *Chem. Eng. Sci.* **2000**, *55*, 3461–3474. [CrossRef]
39. Schulze, K.; Makowski, W.; Chyzy, R. Nickel doped hydrotalcites as catalyst precursors for the partial oxidation of light paraffins. *Appl. Clay Sci.* **2001**, *18*, 59–69. [CrossRef]
40. Reichle, W. Catalytic reactions by thermally activated, synthetic, anionic clay minerals. *J. Catal.* **1985**, *94*, 547–557. [CrossRef]
41. Vaccari, A. Preparation and catalytic properties of cationic and anionic clays. *Catal. Today* **1998**, *41*, 53–71. [CrossRef]
42. Rives, V.; Ulibarri, M.A. Layered double hydroxides (LDH) intercalated with metal coordination compounds and oxometalates. *Coord. Chem. Rev.* **1999**, *181*, 61–120. [CrossRef]
43. Ishihara, Y.; Okabe, S. Effects of cholestyramine and synthetic hydrotalcite on acute gastric or intestinal lesion formation in rats and dogs. *Am. J. Dig. Dis.* **1981**, *26*, 553–560. [CrossRef] [PubMed]
44. Barlattani, M.; Mantera, G.; Fasani, R.; Carosi, M. Efficacy of antacid treatment in peptic ulcerative patients: Therapeutic value of synthetic hydrotalcite (Talcid). *Clin. Trials J.* **1982**, *19*, 359–367.
45. Ookubo, A.; Ooi, K.; Hayashi, H. Hydrotalcites as Potential Adsorbents of Intestinal Phosphate. *J. Pharm. Sci.* **1992**, *81*, 1139–1140. [CrossRef] [PubMed]
46. Rives, V.; Carriazo, D.; Martín, C. Heterogeneous Catalysis by Polyoxometalate-Intercalated Layered Double Hydroxides. In *Pillared Clays and Related Catalysts*; Springer: New York, NY, USA, 2010.
47. Mori, K.; Nakamura, Y.; Kikuchi, I. Modification of poly(vinyl chloride). XLI. Effect of hydrotalcite on the stabilization of poly(vinyl chloride) by 6-anilino-1,3,5-triazine-2,4-dithiol and zinc stearate. *J. Polym. Sci. Part C Polym. Lett.* **1981**, *19*, 623–628. [CrossRef]
48. Van der Ven, L.; van Gemert, M.; Batenburg, L.; Keern, J.; Gielgens, L.; Koster, T.; Fischer, H. On the action of hydrotalcite-like clay materials as stabilizers in polyvinylchloride. *Appl. Clay Sci.* **2000**, *17*, 25–34. [CrossRef]
49. Hermosín, M.; Pavlovic, I.; Ulibarri, M.; Cornejo, J. Hydrotalcite as sorbent for trinitrophenol: Sorption capacity and mechanism. *Water Res.* **1996**, *30*, 171–177. [CrossRef]
50. Cheng, W.; Wan, T.; Wang, X.; Wu, W.; Hu, B. Plasma-grafted polyamine/hydrotalcite as high efficient adsorbents for retention of uranium (VI) from aqueous solutions. *Chem. Eng. J.* **2018**, *342*, 103–111. [CrossRef]
51. Ogata, F.; Ueta, E.; Kawasaki, N. Characteristics of a novel adsorbent Fe–Mg-type hydrotalcite and its adsorption capability of As(III) and Cr(VI) from aqueous solution. *J. Ind. Eng. Chem.* **2018**, *59*, 56–63. [CrossRef]
52. Miyata, S. Anion-Exchange Properties of Hydrotalcite-Like Compounds. *Clays Clay Miner.* **1983**, *31*, 305–311. [CrossRef]
53. Goh, K.-H.; Lim, T.-T.; Dong, Z. Application of layered double hydroxides for removal of oxyanions: A review. *Water Res.* **2008**, *42*, 1343–1368. [CrossRef]
54. Abdelouas, A. Formation of Hydrotalcite-like Compounds During R7T7 Nuclear Waste Glass and Basaltic Glass Alteration. *Clays Clay Miner.* **1994**, *42*, 526–533. [CrossRef]
55. Wang, S.-D.; Scrivener, K.L. Hydration products of alkali activated slag cement. *Cem. Concr. Res.* **1995**, *25*, 561–571. [CrossRef]
56. Faucon, P.; Le Bescop, P.; Adenot, F.; Bonville, P.; Jacquinot, J.; Pineau, F.; Felix, B. Leaching of cement: Study of the surface layer. *Cem. Concr. Res.* **1996**, *26*, 1707–1715. [CrossRef]
57. Paul, M.; Glasser, F. Impact of prolonged warm (85 °C) moist cure on Portland cement paste. *Cem. Concr. Res.* **2000**, *30*, 1869–1877. [CrossRef]
58. Scheidegger, A.M.; Wieland, E.; Scheinost, A.; Dähn, R.; Tits, J.; Spieler, P. Ni phases formed in cement and cement systems under highly alkaline conditions: An XAFS study. *J. Synchrotron Radiat.* **2001**, *8*, 916–918. [CrossRef] [PubMed]
59. Suescum-Morales, D.; Fernández, D.C.; Fernández, J.M.; Jiménez, J.R. The combined effect of CO_2 and calcined hydrotalcite on one-coat limestone mortar properties. *Constr. Build. Mater.* **2021**, *280*, 122532. [CrossRef]
60. He, P.; Shi, C.; Tu, Z.; Poon, C.S.; Zhang, J. Effect of further water curing on compressive strength and microstructure of CO_2-cured concrete. *Cem. Concr. Compos.* **2016**, *72*, 80–88. [CrossRef]
61. Erans, M.; Jeremias, M.; Zheng, L.; Yao, J.G.; Blamey, J.; Manovic, V.; Fennell, P.S.; Anthony, E.J. Pilot testing of enhanced sorbents for calcium looping with cement production. *Appl. Energy* **2018**, *225*, 392–401. [CrossRef]
62. Takehira, K.; Shishido, T.; Shoro, D.; Murakami, K.; Honda, M.; Kawabata, T.; Takaki, K. Preparation of egg-shell type Ni-loaded catalyst by adopting "Memory Effect" of Mg–Al hydrotalcite and its application for CH_4 reforming. *Catal. Commun.* **2004**, *5*, 209–213. [CrossRef]
63. Gao, Z.; Sasaki, K.; Qiu, X. Structural Memory Effect of Mg–Al and Zn–Al layered Double Hydroxides in the Presence of Different Natural Humic Acids: Process and Mechanism. *Langmuir* **2018**, *34*, 5386–5395. [CrossRef]
64. Yong, Z.; Rodrigues, E. Hydrotalcite like compounds as adsorbents for carbon dioxide. *Energy Convers. Manag.* **2002**, *43*, 1865–1876. [CrossRef]
65. Rocha, C.; Soria, M.; Madeira, L.M. Doping of hydrotalcite-based sorbents with different interlayer anions for CO_2 capture. *Sep. Purif. Technol.* **2019**, *235*, 116140. [CrossRef]
66. Qu, Z.; Yu, Q.; Brouwers, H. Relationship between the particle size and dosage of LDHs and concrete resistance against chloride ingress. *Cem. Concr. Res.* **2018**, *105*, 81–90. [CrossRef]
67. Yang, Z.; Fischer, H.; Cerezo, J.; Mol, J.M.C.; Polder, R. Aminobenzoate modified MgAAl hydrotalcites as a novel smart additive of reinforced concrete for anticorrosion applications. *Constr. Build. Mater.* **2013**, *47*, 1436–1443. [CrossRef]

68. Yang, Z.; Fischer, H.; Polder, R. Synthesis and characterization of modified hydrotalcites and their ion exchange characteristics in chloride-rich simulated concrete pore solution. *Cem. Concr. Compos.* **2014**, *47*, 87–93. [CrossRef]
69. Yang, Z.; Fischer, H.; Polder, R. Modified hydrotalcites as a new emerging class of smart additive of reinforced concrete for anticorrosion applications: A literature review. *Mater. Corros.* **2013**, *64*, 1066–1074. [CrossRef]
70. Lozano-Lunar, A.; Álvarez, J.I.; Navarro-Blasco, Í.; Jiménez, J.R.; Fernández-Rodriguez, J.M. Optimisation of mortar with Mg-Al-Hydrotalcite as sustainable management strategy lead waste. *Appl. Clay Sci.* **2021**, *212*, 106218. [CrossRef]
71. Hu, X.; Zhu, X.; Sun, Z. Fireproof performance of the intumescent fire retardant coatings with layered double hydroxides additives. *Constr. Build. Mater.* **2020**, *256*, 119445. [CrossRef]
72. Wu, Y.; Duan, P.; Yan, C. Role of layered double hydroxides in setting, hydration degree, microstructure and compressive strength of cement paste. *Appl. Clay Sci.* **2018**, *158*, 123–131. [CrossRef]
73. Lauermannová, A.-M.; Paterová, I.; Patera, J.; Skrbek, K.; Jankovský, O.; Bartůněk, V. Hydrotalcites in Construction Materials. *Appl. Sci.* **2020**, *10*, 7989. [CrossRef]
74. Gomes, C.; Mir, Z.; Sampaio, R.; Bastos, A.; Tedim, J.; Maia, F.; Rocha, C.; Ferreira, M. Use of ZnAl-Layered Double Hydroxide (LDH) to Extend the Service Life of Reinforced Concrete. *Materials* **2020**, *13*, 1769. [CrossRef] [PubMed]
75. Mir, Z.M.; Bastos, A.; Höche, D.; Zheludkevich, M.L. Recent Advances on the Application of Layered Double Hydroxides in Concrete—A Review. *Materials* **2020**, *13*, 1426. [CrossRef] [PubMed]
76. Cao, L.; Guo, J.; Tian, J.; Xu, Y.; Hu, M.; Wang, M.; Fan, J. Preparation of Ca/Al-Layered Double Hydroxide and the influence of their structure on early strength of cement. *Constr. Build. Mater.* **2018**, *184*, 203–214. [CrossRef]
77. Long, W.-J.; Xie, J.; Zhang, X.; Fang, Y.; Khayat, K.H. Hydration and microstructure of calcined hydrotalcite activated high-volume fly ash cementitious composite. *Cem. Concr. Compos.* **2021**, *123*, 104213. [CrossRef]
78. Long, W.; Xie, J.; Zhang, X.; Kou, S.; Xing, F.; He, C. Accelerating effect of calcined hydrotalcite-Na_2SO_4 binary system on hydration of high volume fly ash cement. *Constr. Build. Mater.* **2022**, *328*, 127068. [CrossRef]
79. Ma, J.; Duan, P.; Ren, D.; Zhou, W. Effects of layered double hydroxides incorporation on carbonation resistance of cementitious materials. *J. Mater. Res. Technol.* **2019**, *8*, 292–298. [CrossRef]
80. Vágvölgyi, V.; Palmer, S.J.; Kristóf, J.; Frost, R.L.; Horváth, E. Mechanism for hydrotalcite decomposition: A controlled rate thermal analysis study. *J. Colloid Interface Sci.* **2007**, *318*, 302–308. [CrossRef]
81. Yahyaoui, R.; Jimenez, P.E.S.; Maqueda, L.A.P.; Nahdi, K.; Luque, J.M.C. Synthesis, characterization and combined kinetic analysis of thermal decomposition of hydrotalcite ($Mg_6Al_2(OH)_{16}CO_3{\cdot}4H_2O$). *Thermochim. Acta* **2018**, *667*, 177–184. [CrossRef]
82. Miyata, S. Physico-Chemical Properties of Synthetic Hydrotalcites in Relation to Composition. *Clays Clay Miner.* **1980**, *28*, 50–56. [CrossRef]
83. Kannan, V.R.S.; Velu, S. Synthesis and physicochemical properties of cobalt aluminium hydrotalcites. *J. Mater. Sci.* **1995**, *30*, 1462–1468. [CrossRef]
84. Cocheci, L.; Barvinschi, P.; Pode, R.; Popovici, E.; Seftel, E.M. Structural Characterization of Some Mg/Zn-Al Type Hy-drotalcites Prepared for Chromate Sorption from Wastewater. *Chem. Bull.* **2010**, *55*, 40–45.
85. Palmer, S.J.; Spratt, H.J.; Frost, R.L. Thermal decompostition of hydrotalcites with variable cationic ratios. *J. Therm. Anal. Calorim.* **2009**, *95*, 123–129. [CrossRef]
86. Garcia-Gallastegui, A.; Iruretagoyena, D.; Gouvea, V.; Mokhtar, M.; Asiri, A.M.; Basahel, S.N.; Al-Thabaiti, S.A.; Alyoubi, A.O.; Chadwick, D.; Shaffer, M.S.P. Graphene Oxide as Support for Layered Double Hydroxides: Enhancing the CO_2 Adsorption Capacity. *Chem. Mater.* **2012**, *24*, 4531–4539. [CrossRef]
87. Ram Reddy, M.K.; Xu, Z.P.; Lu, G.Q.; Diniz da Costa, J.C. Layered Double Hydroxides for CO_2 Capture: Structure Evolution and Regeneration. *Ind. Eng. Chem. Res.* **2006**, *45*, 7504–7509. [CrossRef]
88. Wang, Q.; Wu, Z.; Tay, H.H.; Chen, L.; Liu, Y.; Chang, J.; Zhong, Z.; Luo, J.; Borgna, A. High temperature adsorption of CO_2 on Mg–Al hydrotalcite: Effect of the charge compensating anions and the synthesis pH. *Catal. Today* **2011**, *164*, 198–203. [CrossRef]
89. Hibino, T. Decarbonation Behavior of Mg-Al-CO_3 Hydrotalcite-like Compounds during Heat Treatment. *Clays Clay Miner.* **1995**, *43*, 427–432. [CrossRef]
90. Tao, Q.; Zhang, Y.; Zhang, X.; Yuan, P.; He, H. Synthesis and characterization of layered double hydroxides with a high aspect ratio. *J. Solid State Chem.* **2006**, *179*, 708–715. [CrossRef]
91. Garcés-Polo, S.; Villarroel-Rocha, J.; Sapag, K.; Korili, S.; Gil, A. Adsorption of CO_2 on mixed oxides derived from hydrotalcites at several temperatures and high pressures. *Chem. Eng. J.* **2018**, *332*, 24–32. [CrossRef]
92. Martunus; Othman, M.R.; Fernando, W.J.N. Elevated temperature carbon dioxide capture via reinforced metal hydrotalcite. *Microporous Mesoporous Mater.* **2011**, *138*, 110–117. [CrossRef]
93. Aschenbrenner, O.; McGuire, P.; Alsamaq, S.; Wang, J.; Supasitmongkol, S.; Al-Duri, B.; Styring, P.; Wood, J. Adsorption of carbon dioxide on hydrotalcite-like compounds of different compositions. *Chem. Eng. Res. Des.* **2011**, *89*, 1711–1721. [CrossRef]
94. Forano, C.T.-G.C.; Hibino, T.; Leroux, F. Layered double hydroxides. In *Hand-Book of Clay Science*; Bergaya, F., Theng, B.K.G., Lagaly, G., Eds.; Elsevier: Newnes, Australia, 2006; ISBN 978-0-08-044183-2.
95. Cai, P.; Zheng, H.; Wang, C.; Ma, H.; Hu, J.; Pu, Y.; Liang, P. Competitive adsorption characteristics of fluoride and phosphate on calcined Mg–Al–CO3 layered double hydroxides. *J. Hazard. Mater.* **2012**, *213–214*, 100–108. [CrossRef] [PubMed]
96. Geng, C.; Xu, T.; Li, Y.; Chang, Z.; Sun, X.; Lei, X. Effect of synthesis method on selective adsorption of thiosulfate by calcined MgAl-layered double hydroxides. *Chem. Eng. J.* **2013**, *232*, 510–518. [CrossRef]

97. Hobbs, C.; Jaskaniec, S.; McCarthy, E.K.; Downing, C.; Opelt, K.; Güth, K.; Shmeliov, A.; Mourad, M.C.D.; Mandel, K.; Nicolosi, V. Structural transformation of layered double hydroxides: An in situ TEM analysis. *npj 2D Mater. Appl.* **2018**, *2*, 4. [CrossRef]
98. Luo, S.; Guo, Y.; Yang, Y.; Zhou, X.; Peng, L.; Wu, X.; Zeng, Q. Synthesis of calcined La-doped layered double hydroxides and application on simultaneously removal of arsenate and fluoride. *J. Solid State Chem.* **2019**, *275*, 197–205. [CrossRef]
99. Elhalil, A.; Qourzal, S.; Mahjoubi, F.; Elmoubarki, R.; Farnane, M.; Tounsadi, H.; Sadiq, M.; Abdennouri, M.; Barka, N. Defluoridation of groundwater by calcined Mg/Al layered double hydroxide. *Emerg. Contam.* **2016**, *2*, 42–48. [CrossRef]
100. Harizi, I.; Chebli, D.; Bouguettoucha, A.; Rohani, S.; Amrane, A. A New Mg–Al–Cu–Fe-LDH Composite to Enhance the Adsorption of Acid Red 66 Dye: Characterization, Kinetics and Isotherm Analysis. *Arab. J. Sci. Eng.* **2018**, *44*, 5245–5261. [CrossRef]
101. Chebli, D.; Bouguettoucha, A.; Reffas, A.; Tiar, C.; Boutahala, M.; Gulyas, H.; Amrane, A. Removal of the anionic dye Biebrich scarlet from water by adsorption to calcined and non-calcined Mg–Al layered double hydroxides. *Desalin. Water Treat.* **2016**, *57*, 22061–22073. [CrossRef]
102. Li, R.; Zhan, W.; Song, Y.; Lan, J.; Guo, L.; Zhang, T.C.; Du, D. Template-free synthesis of an eco-friendly flower-like Mg/Al/Fe-CLDH for efficient arsenate removal from aqueous solutions. *Sep. Purif. Technol.* **2021**, *282*, 120011. [CrossRef]
103. Liu, T.; Chen, Y.; Yu, Q.; Fan, J.; Brouwers, H. Effect of MgO, Mg-Al-NO3 LDH and calcined LDH-CO3 on chloride resistance of alkali activated fly ash and slag blends. *Constr. Build. Mater.* **2020**, *250*, 118865. [CrossRef]
104. Singh, R.; Reddy, M.R.; Wilson, S.; Joshi, K.; da Costa, J.C.D.; Webley, P. High temperature materials for CO_2 capture. *Energy Procedia* **2009**, *1*, 623–630. [CrossRef]
105. Ebner, A.D.; Reynolds, S.P.; Ritter, J.A. Nonequilibrium Kinetic Model That Describes the Reversible Adsorption and Desorption Behavior of CO_2 in a K-Promoted Hydrotalcite-like Compound. *Ind. Eng. Chem. Res.* **2007**, *46*, 1737–1744. [CrossRef]
106. Wang, Q.; Tay, H.H.; Guo, Z.; Chen, L.; Liu, Y.; Chang, J.; Zhong, Z.; Luo, J.; Borgna, A. Morphology and composition controllable synthesis of Mg–Al–CO_3 hydrotalcites by tuning the synthesis pH and the CO_2 capture capacity. *Appl. Clay Sci.* **2012**, *55*, 18–26. [CrossRef]
107. Yong, Z.; Mata, V.; Rodrigues, E. Adsorption of Carbon Dioxide onto Hydrotalcite-like Compounds (HTlcs) at High Temperatures. *Ind. Eng. Chem. Res.* **2001**, *40*, 204–209. [CrossRef]
108. Yang, W.; Kim, Y.; Liu, P.K.T.; Sahimi, M.; Tsotsis, T.T. A study by in situ techniques of the thermal evolution of the structure of a Mg–Al–CO_3 layered double hydroxide. *Chem. Eng. Sci.* **2002**, *57*, 2945–2953. [CrossRef]
109. Peng, J.; Iruretagoyena, D.; Chadwick, D. Hydrotalcite/SBA15 composites for pre-combustion CO_2 capture: CO_2 adsorption characteristics. *J. CO2 Util.* **2018**, *24*, 73–80. [CrossRef]
110. Kim, S.; Jeon, S.G.; Lee, K.B. High-Temperature CO_2 Sorption on Hydrotalcite Having a High Mg/Al Molar Ratio. *ACS Appl. Mater. Interfaces* **2016**, *8*, 5763–5767. [CrossRef]
111. Macedo, M.S.; Soria, M.; Madeira, L.M. High temperature CO_2 sorption using mixed oxides with different Mg/Al molar ratios and synthesis pH. *Chem. Eng. J.* **2021**, *420*, 129731. [CrossRef]
112. Silva, J.; Trujillano, R.; Rives, V.; Soria, M.; Madeira, L.M. High temperature CO_2 sorption over modified hydrotalcites. *Chem. Eng. J.* **2017**, *325*, 25–34. [CrossRef]
113. Gao, Y.; Zhang, Z.; Wu, J.; Yi, X.; Zheng, A.; Umar, A.; O'Hare, D.; Wang, Q. Comprehensive investigation of CO_2 adsorption on Mg–Al–CO3 LDH-derived mixed metal oxides. *J. Mater. Chem. A* **2013**, *1*, 12782–12790. [CrossRef]
114. Walspurger, S.; de Munck, S.; Cobden, P.; Haije, W.; Brink, R.V.D.; Safonova, O. Correlation between structural rearrangement of hydrotalcite-type materials and CO_2 sorption processes under pre-combustion decarbonisation conditions. *Energy Procedia* **2011**, *4*, 1162–1167. [CrossRef]
115. Wang, Q.; Tay, H.H.; Zhong, Z.; Luo, J.; Borgna, A. Synthesis of high-temperature CO_2 adsorbents from organo-layered double hydroxides with markedly improved CO_2 capture capacity. *Energy Environ. Sci.* **2012**, *5*, 7526–7530. [CrossRef]
116. Li, S.; Shi, Y.; Yang, Y.; Zheng, Y.; Cai, N. High-Performance CO_2 Adsorbent from Interlayer Potassium-Promoted Stearate-Pillared Hydrotalcite Precursors. *Energy Fuels* **2013**, *27*, 5352–5358. [CrossRef]
117. Hanif, A.; Dasgupta, S.; Divekar, S.; Arya, A.; Garg, M.O.; Nanoti, A. A study on high temperature CO_2 capture by improved hydrotalcite sorbents. *Chem. Eng. J.* **2014**, *236*, 91–99. [CrossRef]
118. Wang, Q.; O'Hare, D. Recent Advances in the Synthesis and Application of Layered Double Hydroxide (LDH) Nanosheets. *Chem. Rev.* **2012**, *112*, 4124–4155. [CrossRef] [PubMed]
119. Wang, Q.; O'Hare, D. Large-scale synthesis of highly dispersed layered double hydroxide powders containing delaminated single layer nanosheets. *Chem. Commun.* **2013**, *49*, 6301–6303. [CrossRef]
120. Othman, M.; Rasid, N.; Fernando, W. Mg–Al hydrotalcite coating on zeolites for improved carbon dioxide adsorption. *Chem. Eng. Sci.* **2006**, *61*, 1555–1560. [CrossRef]
121. Wu, K.; Ye, Q.; Wang, L.; Meng, F.; Dai, H. Mesoporous alumina-supported layered double hydroxides for efficient CO_2 capture. *J. CO2 Util.* **2022**, *60*, 101982. [CrossRef]
122. Zhu, X.; Chen, C.; Suo, H.; Wang, Q.; Shi, Y.; O'Hare, D.; Cai, N. Synthesis of elevated temperature CO_2 adsorbents from aqueous miscible organic-layered double hydroxides. *Energy* **2018**, *167*, 960–969. [CrossRef]
123. Meis, N.N.A.H.; Bitter, J.H.; de Jong, K.P. On the Influence and Role of Alkali Metals on Supported and Unsupported Activated Hydrotalcites for CO_2 Sorption. *Ind. Eng. Chem. Res.* **2010**, *49*, 8086–8093. [CrossRef]

124. Yavuz, C.T.; Shinall, B.D.; Iretskii, A.V.; White, M.G.; Golden, T.; Atilhan, M.; Ford, P.C.; Stucky, G.D. Markedly Improved CO_2 Capture Efficiency and Stability of Gallium Substituted Hydrotalcites at Elevated Temperatures. *Chem. Mater.* **2009**, *21*, 3473–3475. [CrossRef]
125. Lwin, Y.; Abdullah, F. High temperature adsorption of carbon dioxide on Cu–Al hydrotalcite-derived mixed oxides: Kinetics and equilibria by thermogravimetry. *J. Therm. Anal.* **2009**, *97*, 885–889. [CrossRef]
126. Raki, L.; Beaudoin, J.; Mitchell, L. Layered double hydroxide-like materials: Nanocomposites for use in concrete. *Cem. Concr. Res.* **2004**, *34*, 1717–1724. [CrossRef]